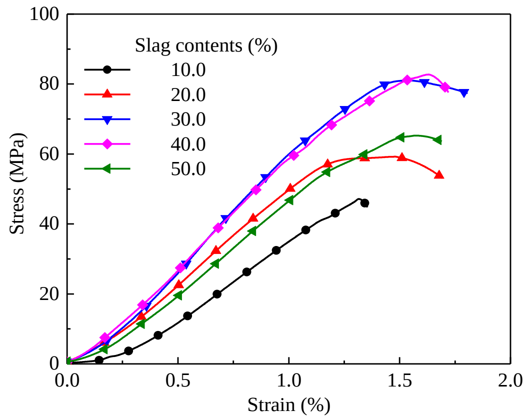

(b) -1.0 °C

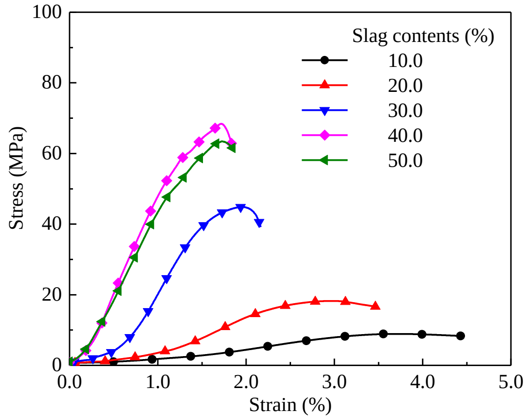

(c) -20.0 °C

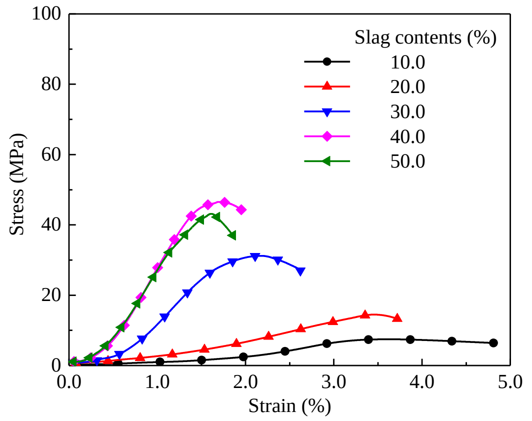

(d) -40.0 °C

Fig.6 The quasi-static compressive stress-stain curves of geopolymer with different slag contents after freeze-thaw cycles at different freezing temperatures.

Fig.7 (a) and (b) further show the relationship between ultimate compressive strength and elasticity modulus of geopolymer composites and slag contents after freeze-thaw cycles at different freezing temperatures. The elastic modulus is calculated from the elastic rising slope of the stress-strain curve. As shown in Fig.7 (a), the ultimate compressive strength of geopolymer composites after curing for 28 days firstly increases and then decreases as the slag content increases. The geopolymer with 40.0% slag content exhibits the highest compressive strength, reaching 87.5 MPa. This indicates that the incorporation of slag can improve the mechanical properties of geopolymer, while excessive slag content reduces the mechanical properties, which is consistent with previous studies (Hanssan and Ismail, 2018). In addition, after freeze-thaw cycles at a freezing temperature of -1.0 °C, the ultimate compressive strengths of geopolymer with different slag contents all decrease slightly. However, when the freezing temperature is -20.0 °C, the ultimate compressive strength of geopolymer composites with 10.0% slag content decreases from 50.7 MPa to 8.9 MPa. Meanwhile, the ultimate compressive strength of geopolymer composites increases gradually as the slag content increases. When the slag content is 50.0%, the ultimate compressive strength of geopolymer composites only decreases by 6.0 MPa, which is 63.4 MPa. As the freezing temperature continues to decrease, the ultimate compressive strengths of geopolymer composites all decrease significantly after freeze-thaw cycles at a freezing temperature of -40.0 °C, which is consistent with the large number of cracks shown in Fig.4. The tendency of the elasticity modulus of geopolymer after freeze-thaw cycles at different freezing temperatures is similar to that of ultimate compressive strength, which first increases and then decreases as the slag content increases. Meanwhile, under the same slag contents, the elasticity modulus of the geopolymer decreases gradually as the freezing temperature decreases.

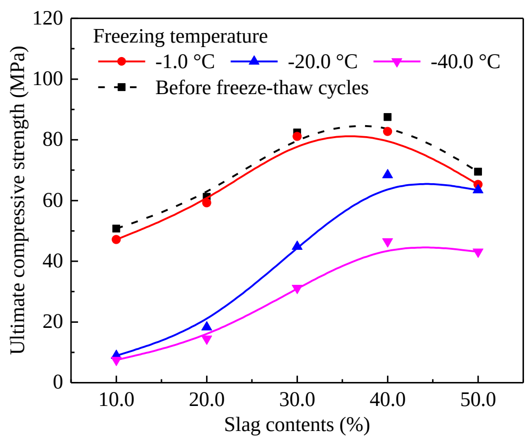

(a)

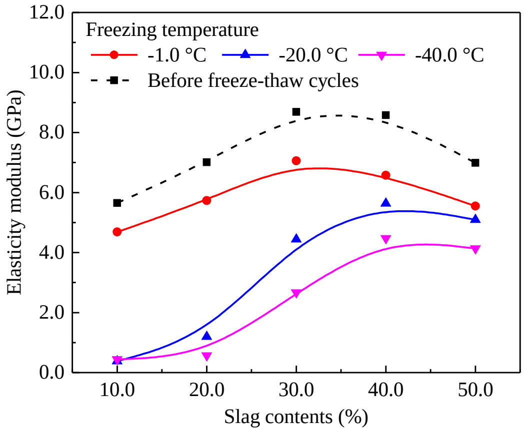

(b)

Fig.7 The relationship between ultimate compressive strength (a) and elasticity modulus (b) of geopolymer specimens and slag contents after freeze-thaw cycles at different freezing temperatures.

Fig.8 (a) shows the effect of the freezing temperature on the strength loss ratio of geopolymers with different slag contents. As shown in Fig.8 (a), the strength loss ratios of geopolymer composites with different slag content all increase significantly as the freezing temperature decreases. After freeze-thaw cycles at a freezing temperature of -1.0 °C, the strength loss ratios of geopolymer with different slag contents are all less than 10%. It indicates that geopolymer composites can maintain relatively stable mechanical properties at a freezing temperature of -1.0 °C. However, when the freezing temperature is -20.0 °C, the geopolymer composites with different slag contents all show an increasing trend, but the rate of increase differs. Among them, the geopolymer composites with 10.0% slag content show the highest strength loss ratio, which is 82.4%. The strength loss ratio of geopolymer composites at a freezing temperature of -20.0 °C decreases gradually as the slag content increases. When the slag content is 50.0%, the strength loss ratio of geopolymer composites is relatively stable, only increasing by 2.6%. When the freezing temperature is -40.0 °C, the strength loss ratio of geopolymer composites with different slag contents further increases. This indicates that a decrease in freezing temperature can exacerbate freeze-thaw damage. The phenomenon can be further explained by the LF-NMR test results. The phase transformation and migration of geopolymer pore water in cold environments are closely related to the pore structure. Previous studies found that the capillary pores freeze at -12.0 °C. Since the gel pore water molecules are attached to the solid surface, the gel pore water does not freeze above -78.0 °C (Wang et al., 2022). As shown in Fig.2, the pore size in the geopolymer mainly concentrates in the range of 10^{-3} to 10^{-1} μm, which can be divided into gel pore and capillary pore. When the freezing temperature is -1.0 °C, the water in the gel pore and capillary pore is not frozen and thus the physical and mechanical of geopolymer composites remain stable. When the freezing temperature is -20.0 °C, the water in the capillary pore undergoes a phase transformation as the temperature changes, causing damage to the geopolymer. Meanwhile, the capillary pore volume gradually decreases as slag content, increases, resulting in the improvement of freeze-thaw resistance of geopolymer composites.

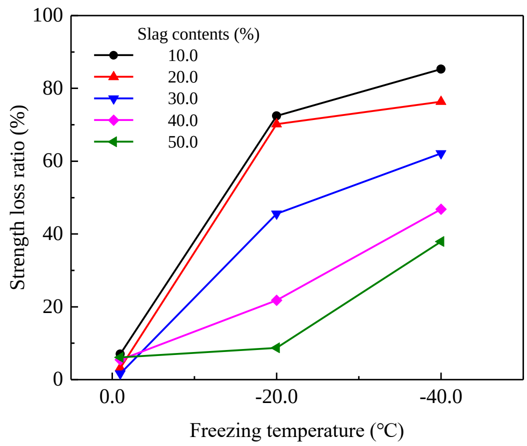

(a)

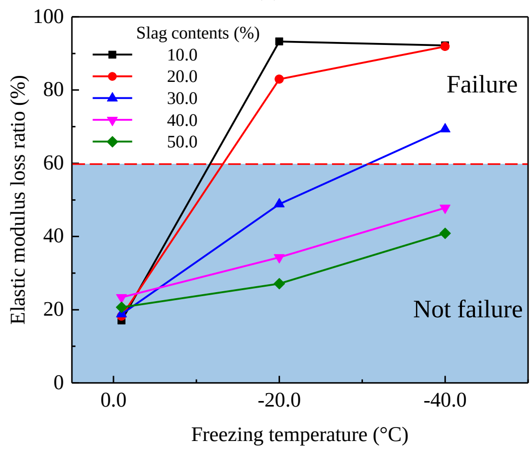

(b)

Fig.8 The effect of the freezing temperature on the strength loss ratio (a) and elastic modulus loss ratio (b) of geopolymer with different slag contents.

Fig.8 (b) shows the effect of the freezing temperature on the elastic modulus loss ratio of geopolymer with different slag contents. As shown in Fig.8 (b), the variation trend of the elastic modulus loss ratio is similar to that of the strength loss ratio as the freezing temperature decreases. The elastic modulus loss ratio increases significantly as the freezing temperature decreases and decreases as the slag content increases. According to GB/T 50082-2009, the specimen is defined as in a failure state when the elastic modulus loss ratio exceeds 60.0%. As shown in Fig.8 (b), when the freezing temperature is -1.0 °C, the elastic modulus loss ratios of geopolymers with 10.0%, 20.0%, 30.0%, 40.0% and 50.0% slag content are all less than 60.0%. When the freezing temperature is -20.0 °C, the elastic modulus loss ratio of geopolymer with 30.0%, 40.0% and 50.0% slag content is less than 60.0%. When the freezing temperature is -40.0 °C, the elastic modulus loss ratio of geopolymer with 40.0% and 50.0% slag content is less than 60.0%. To determine the optimal slag contents, Fig.9 further shows a comprehensive analysis of the compressive strength and elastic modulus of the geopolymer composites after freeze-thaw cycles at different freezing temperatures. As shown in Fig.9, the geopolymer composites with 40.0% and 50.0% slag content still preserve high mechanical properties after freeze-thaw cycles at different freezing temperatures, which are all larger than 40.0 MPa. It indicates that the geopolymer composites with 40.0% and 50.0% slag content can be used as a cementitious material to replace PO 42.5 cement and have potential application prospects in severe cold areas. In addition, the compressive strength and elastic modulus of geopolymer after freeze-thaw cycles in different freezing temperatures can also be observed in Fig.9, which can provide a reference for the application of geopolymers in practical engineering.

Slag contents

Freezing temperature	10.0 %	20.0 %	30.0 %	40.0 %	50.0 %
-1.0 °C	47.15(4.69)	59.23(5.73)	81.05(7.06)	82.71(6.57)	65.25(5.55)
-20.0 °C	8.91(0.38)	18.24(1.19)	44.85(4.44)	68.40(5.63)	63.42(5.10)
-40.0 °C	7.46(0.44)	14.48(0.57)	31.20(2.67)	46.54(4.48)	43.14(4.13)

■ Suggested slag content *σ(E)*: *σ* is compressive strength MPa, *E* is elastic modulus GPa.

Fig.9 Comprehensive analysis of compressive strength and elastic modulus of the geopolymer composites after freeze-thaw cycles at different freezing temperatures.

This paper mainly focuses on investigating the effect of freezing temperature on the physical and mechanical properties of slag-modified metakaolin-based geopolymers and proposes the slag content to satisfy the requirement of practical application in cold regions. The theoretical research of the freeze-thaw mechanism of geopolymer is also in the framework of an overall project and will be further investigated. In addition, the slag-modified metakaolin-based geopolymer in this study is a cementitious material, which can provide a reference for further research on the freeze-thaw resistance of geopolymer mortar and concrete.

4 Conclusions

The present study presents an experimental investigation of optimal slag content for the geopolymer composites under F-T cycles at different freezing temperatures. The following conclusions can be drawn from the current study:

1. The porosity of geopolymer composites decreases as slag content increases, indicating that the incorporation of slag content can significantly compact the geopolymer composites. Meanwhile, the gel pore and transition pore volume proportion all decrease as the slag content increases.

2. The freeze-thaw damage of geopolymer composites is more serious as the freezing temperature decreases, but the damage degree of the geopolymer composites decreases as slag content increases. The width and number of cracks in geopolymer composites after freeze-thaw cycles all decrease as the slag content increases, indicating that the incorporation of slag can inhibit the cracking of the geopolymer in cold environments.

3. The incorporation of the slag can significantly reduce the mass loss ratio and strength loss ratio of geopolymer composites after freeze-thaw cycles and improve the freeze-thaw resistance of geopolymer composites.

4. The geopolymer composites with 40.0% and 50.0% slag content still preserve high mechanical properties after freeze-thaw cycles at different freezing temperatures and have potential application prospects in cold areas.

Acknowledgments

This work is supported by the National Natural Science Foundation of China (No. 51627812).

Author contributions

Lifeng FAN designed the research. Lifeng FAN and Yan XI processed the corresponding data. Guang WANG wrote the first draft of the manuscript. Guang WANG and Weiliang ZHONG helped to organize the manuscript. Lifeng FAN and Weiliang ZHONG revised and edited the final version.

Conflict of interest

Lifeng FAN, Weiliang ZHONG, Guang WANG, and Yan XI declare that they have no conflict of interest.

References

Chen CH, Zhu PH, Wu JY, Yi L, 2014. Research on frost resistance of recycled high performance concrete. *Applied Mechanics and Materials*, 586:1456-1460. https://doi.org/10.4028/www.scientific.net/AMM.584-586.1456

Duxson P, Provis JL, Lukey GC, Deventer JSJV, 2007a. The role of inorganic polymer technology in the development of 'green concrete'. *Cement and Concrete Research*, 37:1590-1597. https://doi.org/10.1016/j.cemconres.2007.08.018

Duxson P, Provis JL, Jimenez AF, Lukey GC, 2007b. Geopolymer technology: the current state of the art. *Journal of Materials Science*, 42:2917-2933. https://doi.org/10.1007/s10853-006-0637-z

Du T, Zhou B, Liu B, Ye H, Peng JL, 2022. The influence of opposite-side high temperature on the frozen behavior of containment concrete under single-side freeze-thaw method. *Structures*, 36:854-863. https://doi.org/10.1016/j.istruc.2021.12.063

Fu Y, Cai L, Yonggen W, 2011. Freeze-thaw cycle test and damage mechanics models of alkali-activated slag concrete. *Construction and Building Materials*, 25:3144-3148. https://doi.org/10.1016/j.conbuildmat.2010.12.006

Fan LF, Zhong WL, Zhang YH, 2022. Effect of the composition and concentration of geopolymer pore solution on the passivation characteristics of reinforcement. *Construction and Building Materials*, 319:126128. https://doi.org/10.1016/j.conbuildmat.2021.126128

Gencel O, Benli A, Bayraktar OY, Kaplan G, Sutcu M, Elabade WAT, 2021. Effect of waste marble powder and rice husk ash on the microstructural, physico-mechanical and transport properties of foam concretes exposed to high temperatures and freeze-thaw cycles. *Construction and Building Materials*, 291:123374. https://doi.org/10.1016/j.conbuildmat.2021.123374

Hanssan H, Ismail, 2018. Effect of process parameters on the performance of fly ash/GGBS bended geopolymer composites. *Journal of Sustainable Cement-Based Materials*, 7:122-140. https://doi.org/10.1080/21650373.2017.1411296

Jacobsen S, Soether D, Sellevold E, 1997. Frost testing of high strength concrete: frost/salt scaling at different cooling rates. *Materials and Structures*, 30:33-42. https://doi.org/10.1007/BF02498738

Jiao ZZ, Li XY, Yu QL, 2021. Effect of curing conditions on freeze-thaw resistance of geopolymer mortars containing various calcium resources. *Construction and Building Materials*, 323:125507. https://doi.org/10.1016/j.conbuildmat.2021.125507

Luukkonen T, Abdollahnejad Z, Yliniemi J, Kinnenen P, Illikainen M, 2018. Comparison of alkali and silica sources in one-part alkali-activated blast furnace slag mortar. *Journal of Cleaner Production*, 187:171-179. https://doi.org/10.1016/j.jclepro.2018.03.202

Liu L, He Z, Cai XH, Fu SJ, 2020. Application of Low-Field NMR to the pore structure of concrete. *Applied Magnetic Resonance*, 2:15-31. https://doi.org/10.1007/s00723-020-01229-7

Nasvi MCM, Ranjith PG, Sanjayan J, 2013. The permeability of geopolymer at downhole stress conditions: application for carbon dioxide sequestration wells. *Applied Energy*, 102:1391-1398. https://doi.org/10.1016/j.apenergy.2012.09.004

Parbhoo B, Nagy O, 1988. Molecular dynamics in hydrogen bond forming environments. The role of hydrophilic-hydrophobic interactions in pyridine-water mixtures. *Journal of Molecular Structure* 177:393-399. https://doi.org/10.1016/0022-2860(88)80104-2

Richardson A, Coventry K, Edmondson V, Dias E, 2016. Crumb rubber used in concrete to provide freeze-thaw protection (optimal particle size). *Journal of Cleaner Production*, 112:599-606. https://doi.org/10.1016/j.jclepro.2015.08.028

Rashad AM, Sadek DM, 2020. Behavior of alkali-activated slag pastes blended with waste rubber powder under the effect of freeze/thaw cycles and severe sulfate attack. *Construction and Building Materials*, 265:120716. https://doi.org/10.1016/j.conbuildmat.2020.120716

Shahrajabian F, Behfarnia K, 2018. The effects of nano particles on freeze and thaw resistance of alkali-activated slag concrete. *Construction and Building Materials*, 176:172-178. https://doi.org/10.1016/j.conbuildmat.2018.05.033

Sahin F, Uysal M, Canpolat O, Cosgun T, Dehghanpore H, 2021a. The effect of polyvinyl fibers on metakaolin-based geopolymer mortar with different aggregate filling. *Construction and Building Materials*, 300:124257. https://doi.org/10.1016/j.conbuildmat.2021.124257

Sahin Y, Akkaya Y, Tasdemir MA, 2021b. Effect of freezing conditions on the frost resistance and microstructure of concrete. *Construction and Building Materials*, 270: 121458. https://doi.org/10.1016/j.conbuildmat.2020.121458

Tian LY, He DP, Zhao JN, Wang HG, 2021. Durability of geopolymers and geopolymer concretes: a review. *Reviews on Advanced Materials Science*, 60:1-14. https://doi.org/10.1515/rams-2021-0002

Wang RJ, Hu ZY, Li Y, Wang K, Zhang H, 2022. Review on the deterioration and approaches to enhance the durability of concrete in the freeze-thaw environment. *Construction and Building Materials*, 321:126371. https://doi.org/10.1016/j.conbuildmat.2022.126371

Xie JH, Wang JJ, Wang CH, Huang PY, Fang C, 2019. Sulfate resistance of recycled aggregate concrete with GGBS and fly ash-based geopolymer. *Materials*, 12:1247. https://doi.org/10.3390/ma12081247

Yang M, Paudla SR, Asa E, 2020. Comparison of pore structure in alkali activated fly ash geopolymer and ordinary concrete due to alkali-silica reaction using micro-computed tomography. *Construction and Building Materials*, 236:117524. https://doi.org/10.1016/j.conbuildmat.2019.117524

Yuan Y, Zhao R, Li R, Wang Y, Cheng Z, Li F, Ma ZJ, 2020. Frost resistance of fiber-reinforced blended slag and Class F fly ash-based geopolymer concrete under the coupling effect of freeze-thaw cycling and axial compressive loading. *Construction and Building Materials*, 250:118831. https://doi.org/10.1016/j.conbuildmat.2020.118831

Zhao R, Yuan Y, Cheng Z, Wen T, Li J, Li F, Ma ZJ, 2019a. Freeze-thaw resistance of Class F fly ash-based geopolymer concrete. *Construction and Building Materials*, 222:474-483. https://doi.org/10.1016/j.conbuildmat.2019.06.166

Zhao M, Zhang G, Htet KW, Kwon M, Liu C, Xu Y, Tao M, 2019b. Freeze-thaw durability of red mud slurry-class F fly ash based geopolymer: Effect of curing condition. *Construction and Building Materials*, 215:381-390. https://doi.org/10.1016/j.conbuildmat.2019.04.235

Zhang A, Yang WC, Ge Y, Wang YZ, Liu PH, 2020a. Study on the hydration and moisture transport of white cement containing nanomaterials by using low field nuclear magnetic resonance. *Construction and Building Materials*, 249:118788. https://doi.org/10.1016/j.conbuildmat.2020.118788

Zhang P, Wang K, Li Q, Wang J, Ling Y, 2020b. Fabrication and engineering properties of concretes based on geopolymers/alkali-activated binders - a review. *Journal of Cleaner Production*, 258:120896. https://doi.org/10.1016/j.jclepro.2020.120896

Zhang BF, Feng Y, Xie JH, Lai DM, Yu T, Huang DC, 2021. Rubberized geopolymer concrete: Dependence of mechanical properties and freeze-thaw resistance on replacement ratio of crumb rubber. *Construction and Building Materials*, 310:125248. https://doi.org/10.1016/j.conbuildmat.2021.125248

Zhu H, Zhai M, Liang G, Li H, Wu Q, Zhang C, Hua S, 2021. Experimental study on the freezing resistance and microstructure of alkali-activated slag in the presence of rice husk ash. *Journal of Building Engineering*, 38:102173. https://doi.org/10.1016/j.jobe.2021.102173

Electronic supplementary materials

Table S1, Figs. S1–S3

中文概要

题　目：不同冻结温度的 F-T 循环作用下地聚物复合材料最佳矿渣掺量研究

作　者：范立峰[1]，钟惟亮[1]，王广[1]，席岩[1]

机　构：[1]北京工业大学，城市建设学部，中国北京，100124

目　的：提高地聚物的抗冻融循环性能对确保地聚物在寒区中的耐久性具有重要意义。本文旨在研究冻结温度对矿渣改性的偏高岭土基地聚物物理和力学性能的影响，以期为地聚物在寒区中的实际应用和耐久性评估提供参考。

创新点：1. 提出了冻融循环条件下地聚物复合材料的最佳矿渣含量；2. 矿渣的掺入可以抑制地聚物在寒冷环境中的开裂，提高地聚物复合材料的抗冻融性。

方　法：1.制备了不同矿渣的纤维增强聚合物并对其开展了三种冻结温度的冻融循环试验；2. 分析了不同矿渣的纤维增强聚合物的孔隙结构特性；3. 分析了冻融循环后不同矿渣的纤维增强聚合物的物理力学性能；4. 提出了冻融循环作用下地聚物复合材料的最佳矿渣含量。

结　论：1. 随着矿渣含量的增加，地聚物复合材料的孔隙率降低，凝胶孔和过渡孔均逐渐减小；2. 冻融循环后，地聚物复合材料中的裂缝宽度和数量都随着矿渣含量的增加而减少，表明矿渣的掺入可以抑制地聚物在寒冷环境中的开裂；3. 矿渣的掺入可以显著降低地聚物复合材料在冻融循环后的质量损失率和强度损失率，并提高地聚物复合材料的抗冻融性；4. 40.0%和 50.0%矿渣含量的地聚物复合材料在冻融循环后仍保持较高的力学性能，具有潜在的应用前景。

关键词：地聚物复合材料；冻融循环；冻结温度；矿渣掺量